

Mass and energy balances in a molten-carbonate fuel cell with internal reforming

S. Freni, M. Aquino and N. Giordano

Istituto C.N.R.-T.A.E., via salita S. Lucia sopra Contesse 39, 98126 Santa Lucia Messina (Italy)

S. Cavallaro

Dipartimento di Chimica Industriale dell'Università di Messina, P.O. Box 29, 98166 Sant'Agata di Messina (Italy)

(Received November 26, 1991; in revised form March 2, 1992)

Abstract

The direct internal reforming molten-carbonate fuel cell (DIR-MCFC) can be proposed as a cogeneration system (heat + electricity). The influence of several operating parameters on the mass and energy balances of a 10 kW power plant has been investigated by using a mathematical model. The temperature, the steam/carbon ratio, the electrical power and the useful heat fraction have been found to be relevant parameters for optimizing both the energy and the exergy efficiencies. The results indicate that the performance of the system is improved at higher temperatures (973 K) and at fuel utilization (U_f) in the range of 45 to 70%. At lower U_f values the system works endothermically, because the steam reforming reaction prevails and for $U_f > 70\%$, a decrease of the efficiencies is produced by the electrode overpotentials and the ohmic losses.

Introduction

The growing world-wide demand for energy has resulted in efforts to develop advanced electrochemical systems with higher electrical efficiency than the traditional power plants [1]. In this regard, the molten-carbonate fuel cell (MCFC) represents one of the most promising systems [2], and several of the most important technical characteristics related to a practical system [3] have been reported.

The overall efficiency of a fuel cell is not limited by the Carnot cycle, and the maximum amount of electrical energy available is given by the change in Gibbs free energy of the electrochemical reaction [4].

One advantage of the MCFC is its high operating temperature, in the range 873–973 K [5], which is sufficient to sustain the endothermic reaction of CH_4 steam reforming. Consequently, a major effort is underway to integrate direct internal reforming (DIR) with MCFCs utilizing natural gas [6]. The low production of pollutants, the compactness, simplicity, and the absence of noise are further advantages of the MCFC.

Another important advantage is that heat rejected by MCFC system can be recovered by a cogeneration bottoming cycle.

The present paper describes a theoretical model for calculating the energy, exergy, and mass balances for a DIR-MCFC, operating with or without a cogeneration bottoming cycle. The model has been used to analyse the optimum operating conditions for a small plant (electric output power: 10 kW). The calculations have been carried out

for the typical MCFC-working conditions reported in the literature [6]. Furthermore, sensitivity analyses have been developed to evaluate the changes to the system as a function of the following parameters: temperature, steam/carbon ratio, total outlet flow, CO₂ selectivity, output electrical and heat power, unreacted fuel flow, and exergy and energy efficiencies. An understanding of these parameters and their relationship is useful for optimizing the overall system performance. The thermal energy necessary to maintain a constant cell temperature and to produce hydrogen by steam reforming is obtained from the electrochemical cell reactions and from the combustion of unreacted fuel. Consequently, thermal management of this waste heat and the heat required for the endothermic steam reaction is a critical issue. In addition, the waste heat can be utilized in a cogeneration application to provide further enhancement in overall system efficiency. These aspects that are considered in this paper.

Derivation of the model

Hydrogen is a very promising fuel because of its clean oxidation reaction (i.e., only H₂O is formed) and high energy density [7]. It can be produced easily by catalytic steam reforming of natural gas, as represented by the reactions [8]:



The mass balances of these reactions are:

$$(F_{\text{CH}_4}^\circ - x) + (F_{\text{H}_2\text{O}}^\circ - x - y) = (x - y) + (3x + y) \quad (1a)$$

$$(x - y) + (F_{\text{H}_2\text{O}}^\circ - x - y) = y + (3x + y) \quad (2a)$$

This process can be integrated in an MCFC provided with a suitable internal reforming (IR) catalyst [9]. This configuration (DIR-MCFC) does not require an external fuel reformer, which gives therefore simplified heat transfer, resulting in improved performance. At the anode, hydrogen is oxidized by the following reaction:



At the cathode the reaction is:



and the overall reaction can be written as:



The CO₂ is consumed in the cathode and is produced in the anode. Its concentration can be different at the two electrodes. The corresponding open-circuit equilibrium cell voltage (V) is determined by the Nernst equation:

$$V = E^\circ + \frac{RT}{nF} \ln \frac{P_{\text{H}_2} P_{\text{O}_2}^{1/2} P_{\text{CO}_2(c)}}{P_{\text{H}_2\text{O}} P_{\text{CO}_2(a)}} \quad (6)$$

The cell voltage under load is obtained if the contributions from the electrode overpotentials and resistance are included:

$$V_0 = V - (\mu_a + \mu_c) - IR_i S_0 \quad (6a)$$

The cathodic (μ_c) and anodic (μ_a) overpotentials and the specific internal resistance (R_i) which were reported by Wilemski [10] were used in this analysis.

According to Mori *et al.* [11], the unknown terms of the above equation can be easily computed by solving the two equilibrium expressions of the eqns. (1) and (2), written as:

$$K_1 = \frac{(x-y)(3x+y-F_{H_2})^3 P^2}{10^{10}(F_{CH_4}^o-x)(F_{H_2O}^o-x-y+F_{H_2})(F_{CH_4}^o+F_{H_2O}^o+F_{H_2}+2x)^2} \quad (7)$$

$$K_2 = \frac{(y+F_{H_2})(3x+y-F_{H_2})}{(x-y)(F_{H_2O}^o-x-y+F_{H_2})} \quad (8)$$

These equations can be used to calculate the outlet gas compositions and the cell voltage (V_0) (accounting for the losses due to the overpotentials and the internal resistance) when the current density is known. Consequently, the output electric power, the heat capacity of the exhaust gases and the energy available from the unreacted fuels (CH_4 , CO and H_2) can be computed. Thus, both electrical and thermal powers, which can contribute to the overall cell efficiency determined.

For such a system, at steady-state condition and with negligible kinetic and potential energies, the energy balance can be written as:

$$m_f h_f + m_o h_o = W + Q_u + \sum_w Q_w + \sum_w m_w h_w \quad (9)$$

This eqn. (9) shows the relationship between the total inlet energy (fuel + oxidant) and the total output electrical and thermal energy (useful + waste). For a MCFC plant that is integrated with a cogeneration device, the thermal energy is generated by the cell electrochemical reaction, ohmic resistance and combustion of the unreacted fuel ($CH_4 + CO + H_2$), but in practice only a fraction (f) of it can be used. Thus, the theoretical efficiency can be calculated as:

$$\eta = \frac{W + Q_u}{m_f h_f} = \frac{W + f Q_p}{m_f h_f} \quad (10)$$

Moreover, it is meaningful to calculate the exergy efficiency, which considers the temperature of the output released energy. This parameter can be expressed by the following equation:

$$\phi = \frac{W + Q_u(1 - T_0/T_p)}{m_f \epsilon_f} = \frac{W + f Q_p(1 - T_0/T_p)}{\alpha_E m_f h_f} \quad (11)$$

In eqn. (11), the reference temperature (T_0) is conventionally fixed at 298 K [12].

Standard base line condition and evaluation parameters

The model has been used to analyse an DIR-MCFC cogenerated power plant of small size (electric output power: 10 kW). As a base-line condition, the calculations have been carried out for the typical working conditions reported in the literature [5, 13] and summarized in Table 1. Furthermore, sensitivity analysis has been developed to evaluate the behaviour of the system, considering the following parameters:

- steam/carbon (S/C) ratio which represents the ratio of the amount of inlet water vapour to methane;
- total outlet flow is defined as the sum of the anode (CH_4 , CO , CO_2 , H_2 and H_2O) and cathode (N_2 , O_2 and CO_2) gas flows;

TABLE 1

Standard operating condition (base line)

Cell temperature (T_p)	923 K
Pressure	0.1 MPa
Electrical power (W)	10 kW
Current density (I)	150 mA/cm ²
Cell number	20 cells
Effective area (per cell)	5016 cm ²
Fuel utilization (U_f)	60%
Molar steam/carbon ratio (S/C)	2.0
Oxidant utilization (U_{ox})	36.2%
O ₂ /CO ₂ molar fraction	0.1672/0.2
Specific internal resistance (R_i)	0.8 Ω cm ²

- CO₂ selectivity is defined by the ratio between the molar fraction of the output CO₂ and the sum of the molar fractions of CO and CO₂;
- electrical power is the product of the total output current and the cell voltage;
- unreacted fuel flow evaluated as the sum of the single flows of unreacted fuels (CO, H₂ and CH₄);
- energy efficiency defined as the ratio between the energy output and the energy input;
- exergy efficiency defined as the energy efficiency multiplied by a factor that takes into account the temperatures of the system.

Results

The evaluation carried out for a 10 kW DIR-MCFC stack at the base-line condition specified in Table 1 gives an electrical efficiency of 32.8%. The final value of methane conversion is 99.1% and the CO₂ selectivity is 81.5%. At this operating condition, the unreacted hydrogen content in the exhaust fuel gas flow is equal to 12.7%, corresponding to 109.7 mol/h.

Starting from these results, the further calculations have shown the sensitivity of the system to the main working parameters. The first parameter that was evaluated is the total outlet flow* as a function of the electric power, for S/C ratios of 1.5, 2.0 and 2.5 and temperatures of 873, 923 and 973 K. The total outlet flow is not very sensitive to the cell temperature. In fact, only small differences of less than 2.5% in the outlet flow rates are observed when the cell is at open circuit or is operating at limited power (up to 8 kW), as shown in Fig. 1. Its dependence on the S/C ratio is greater because the total outlet flow increases by about 10% on changing the S/C ratio from 1.5 to 2.5. The flow decreases slightly when the output power increases (Fig. 2(a)). The total outlet flow rate of the cell is nearly constant at different output powers, however the anodic and cathodic outlet flows are strongly influenced by the power. This trend is shown in Fig. 2(b), where it is evident that an electrical power of 10 kW corresponds to outlet flows of 864 mol/h for the anode and 1899 mol/h for the cathode, compared to 490 mol/h and 2320 mol/h, respectively, for the same cell at open circuit.

*The analysis considers the outlet flow because all of the waste heat is removed by the flow of outlet gases from the cell, i.e., there is no additional cell cooling.

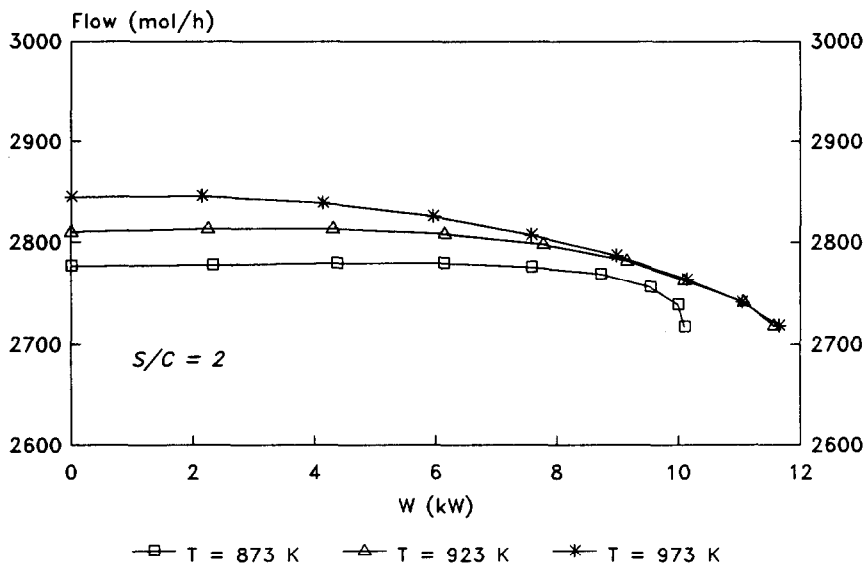
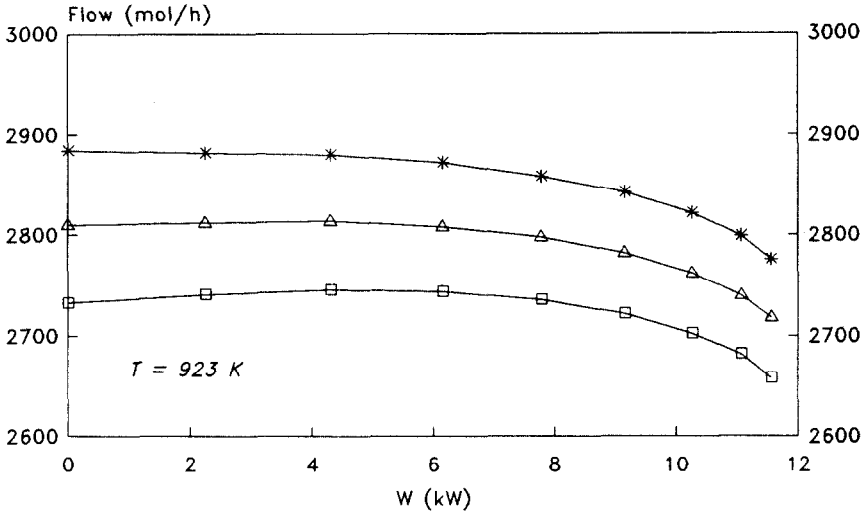


Fig. 1. Total outlet flow vs. electrical power at $S/C=2$.

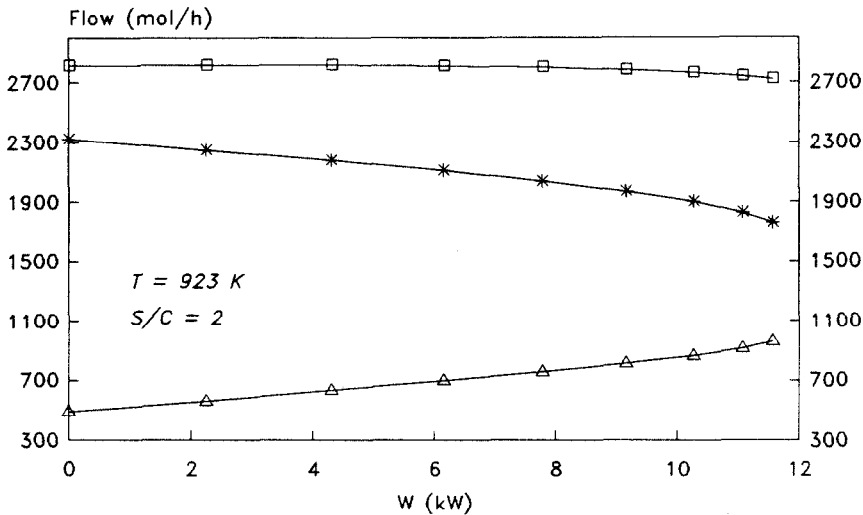
The CH_4 conversion and the exhaust fuel composition depend mainly on the current, temperature and S/C ratio. The dependence of these factors is shown in Table 2 for a MCFC operating at $U_f=60\%$. The exhaust fuel composition is calculated for different cases. The amount of unconverted CH_4 is minimal for the three cell temperatures, and a decrease of 100 K (from 973 to 873 K) does not significantly change the CH_4 conversion. However, the equilibrium of the shift reaction is strongly influenced by the temperature and S/C ratio. In fact, the content of unconverted CO varies from 6.8% at 873 K, to 9.8% at 973 K. Increasing the S/C ratio from 1.5 to 2.5 enhances the formation of products and the unreacted fuel ($\text{CO} + \text{CH}_4$) is minimized. For instance, at $U_f=60\%$ and $T=923$ K, for $S/C=2.5$, the $\text{CH}_4 + \text{CO}$ molar fractions represent only 7.5% of the total outlet gas mixture, while for $S/C=1.5$ it corresponds to 10.1%.

The variation of the exhaust fuel composition with the output electrical power of a system working at 923 K and $S/C=2.0$, is summarized in Fig. 3, where plots of CH_4 , CO, H_2 , H_2O and CO_2 versus W are reported. The CH_4 conversion increases with the electrical power from 59.5% at open circuit up to 99.1% at $W=10$ kW. The H_2O content increases with the power, reaching the value of 41.2% (356 mol/h) at 10 kW. The amount of CO in the exhaust fuel reaches a maximum for the electrical power of 6 kW. It falls at higher electrical power (i.e., at $W=10$ kW the amount of CO is 73 mol/h).

Table 3 illustrates the selectivity to CO_2 as a function of the electrical power, calculated for S/C ratios varying from 1.5 to 2.5 and T from 873 to 973 K. The CO_2 selectivity is more strongly influenced by the temperature than by the S/C ratio, and mainly when the system is at low power. At $U_f=40\%$ and 873 K, the CO_2 selectivity is equal to 78.0% but decreases to 64.8% at 973 K. When the system is operating at close to its highest electrical power, the production of CO_2 is almost the same at the



(a) \square S/C = 1.5 \triangle S/C = 2 $*$ S/C = 2.5



(b) \square Total \triangle Anodic $*$ Cathodic

Fig. 2. (a) Total outlet flow vs. electrical power at $T=923\text{ K}$; (b) total, anodic and cathodic outlet flows vs. electrical power at base line conditions (Table 1).

three temperatures. The calculations indicate the highest value of selectivity ($\approx 90\%$) at $U_f=80\%$, with an unreacted CO stream (4.3%) of 41.2 mol/h.

Figure 4(a) shows the correlation of the energy/exergy efficiencies and the electrical power for three values of the useful heat fraction (f). The curve for $f=0$ represents a MCFC system used to produce electric energy only. In this case, the heat available in the system is not recovered, except to sustain the internal reforming reaction. By

TABLE 2

Exhaust fuel composition at $U_f=60\%$

Temperature (K)	S/C	R_i ($\Omega \text{ cm}^2$)	μ (mV)	W (kW)	CH ₄ (%)	CO (%)	H ₂ (%)	H ₂ O (%)	CO ₂ (%)
873	2.0	0.6	195	9.3	0.5	6.8	13.0	40.6	39.1
873	2.0	0.8	156	9.4	0.5	6.8	13.0	40.6	39.1
873	2.0	0.8	195	8.4	0.5	6.8	13.0	40.6	39.1
873	2.0	0.8	234	8.2	0.5	6.8	13.0	40.6	39.1
873	2.0	1.0	195	8.4	0.5	6.8	13.0	40.6	39.1
923	1.5	0.8	129	9.5	0.2	9.9	12.8	37.8	39.4
923	2.0	0.6	129	9.9	0.1	8.5	12.7	41.2	37.4
923	2.0	0.8	103	9.9	0.1	8.5	12.7	41.2	37.4
923	2.0	0.8	129	9.5	0.1	8.5	12.7	41.2	37.4
923	2.0	0.8	155	9.1	0.1	8.5	12.7	41.2	37.4
923	2.0	1.0	129	9.0	0.1	8.5	12.7	41.2	37.4
923	2.5	0.8	129	9.5	0.1	7.4	12.5	44.4	35.6
973	2.0	0.6	94	10.1	0.0	9.8	11.8	42.3	36.2
973	2.0	0.8	75	9.9	0.0	9.8	11.8	42.3	36.2
973	2.0	0.8	94	9.6	0.0	9.8	11.8	42.3	36.2
973	2.0	0.8	113	9.4	0.0	9.8	11.8	42.3	36.2
973	2.0	1.0	94	9.2	0.0	9.8	11.8	42.3	36.2

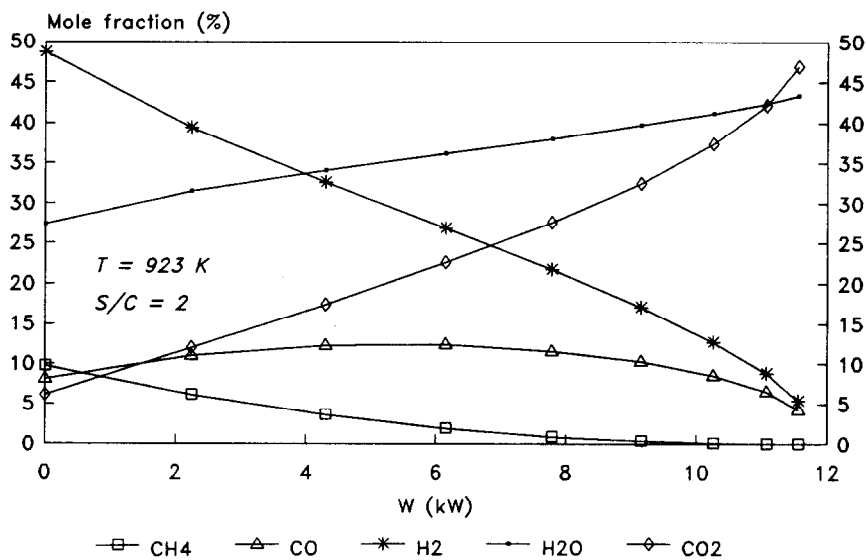


Fig. 3. Exhaust fuel composition vs. electrical power.

definition, the theoretical energy efficiency is equal to 32.8% when the system operates at the base line condition. The condition where the total heat available in the system is used (cogeneration bottoming cycle), corresponds to the curves for $f=1$. The theoretical energy efficiency is equal to 97.2%, but it is not achievable in a practical system.

TABLE 3

CO₂ selectivity at different electrical power (W)

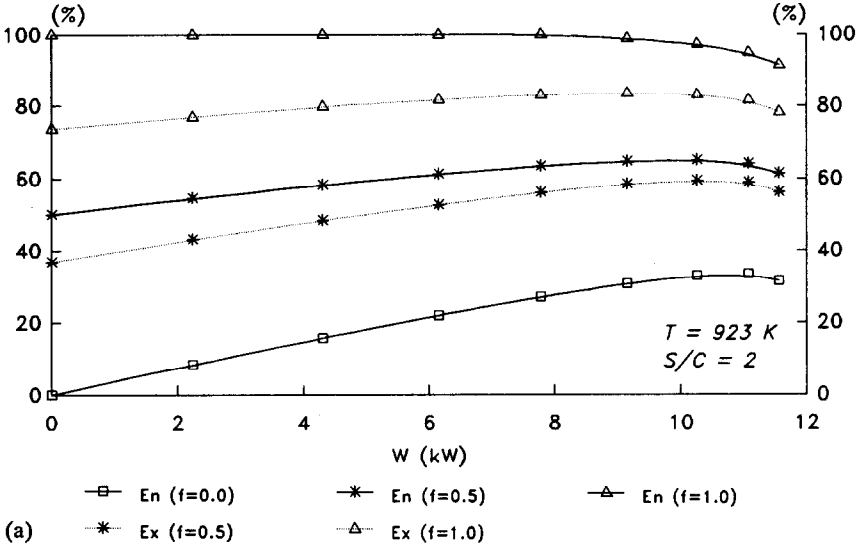
Temperature (K)	S/C	U_f (%)	W (kW)	CO ₂ selectivity (%)
873	2.0	40	7.3	78.0
873	2.0	60	8.4	85.1
873	2.0	80	7.3	92.9
923	1.5	40	7.8	68.0
923	1.5	60	9.5	80.0
923	1.5	80	9.1	90.9
923	2.0	40	7.8	70.3
923	2.0	60	9.5	81.5
923	2.0	80	9.1	91.5
923	2.5	40	7.8	72.3
923	2.5	60	9.5	82.8
923	2.5	80	9.1	92.1
973	2.0	40	7.8	64.8
973	2.0	60	9.6	78.7
973	2.0	80	9.4	90.4

In a real system, the corresponding exergy efficiency is more meaningful because it considers also the thermal level of the several heat contributions. For the examined case it reaches a total value of 83.0%, this being the sum of the contributions of the electrical and thermal energy. A more detailed description of the single contributions of the total output available energy as a function of the useful heat fraction is reported in Fig. 4(b). The behaviour of the electrical and thermal power contributions, achievable for a system operating at 923 K, $S/C=2$ and calculated for fuel utilization (U_f) varying from 0 to 80%, are reported in Figs. 5(a) and 5(b) ($f=0.5$ and 1.0, respectively).

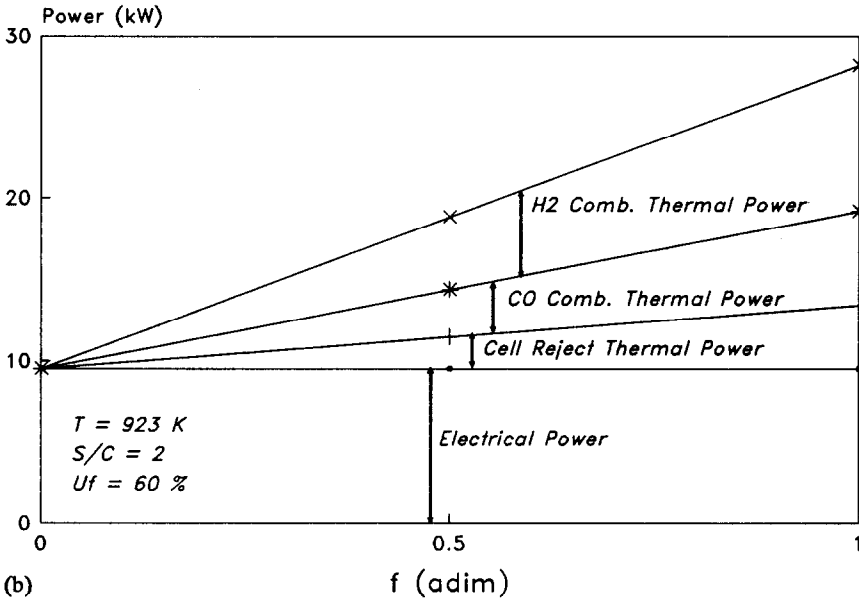
Discussion

Preliminary considerations on the influence of the total outlet flows on the behaviour of a MCFC system have been examined. This parameter is directly correlated to the thermal energy density of the system and it determines to the heat exchangers sizing. As shown in Figs. 1 and 2, the total outlet flow is slightly influenced by the electric power (W) and by the temperature (T), but only the S/C ratio has a significant influence on its final value. These results could seem in disagreement with the fact that higher temperatures or output powers move the equilibrium of the eqn. (1) to the formation of products, increasing the gases total volume. In practice, the outlet flow is given by the contribution of the anodic and the cathodic outlet flows, that show (see Fig. 2(b)) opposite trends. In fact, when the system is under load, the hydrogen oxidation involves the corresponding consumption of a greater volume of the cathodic reactants. At least, highest utilizations give a better balance of the anode and cathode flows, which should reduce the pressure difference between the anodic and cathodic compartments.

As reported in Fig. 3, the CH₄ conversion reaches 85.0% also at open circuit and it increases to 99.0% when a load higher than 8 kW is applied to the system. The CO and hydrogen content in the waste gases represent a significant percentage (about



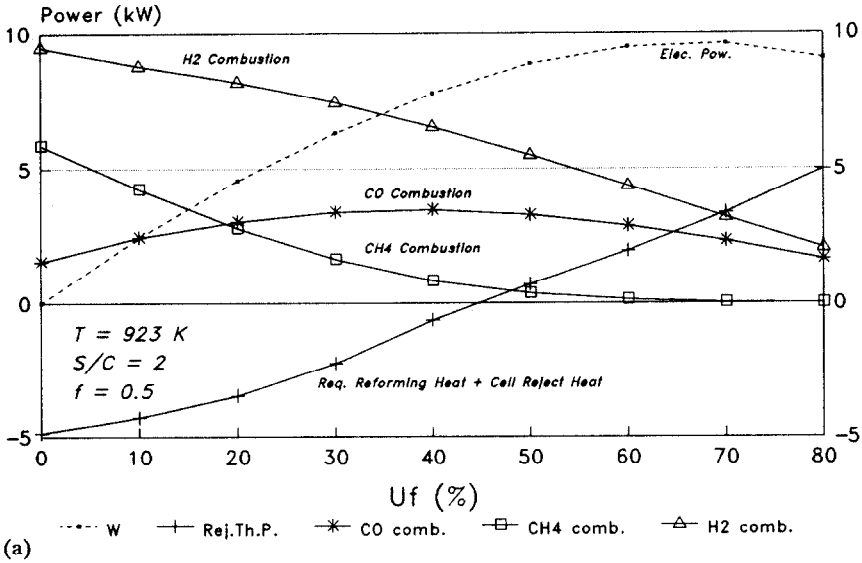
(a)



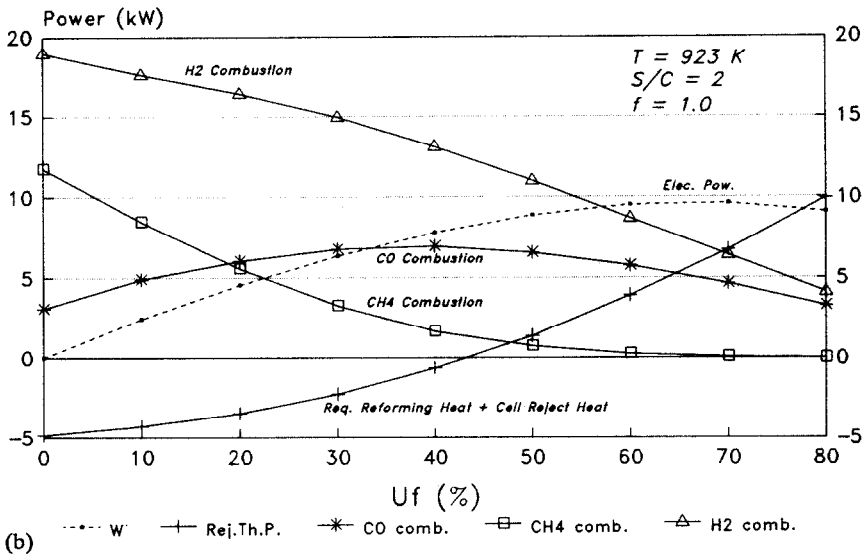
(b)

Fig. 4. (a) Energy and exergy efficiencies vs. electrical power at base line conditions (Table 1); (b) output power vs. useful heat fraction at base line conditions (Table 1).

6 and 11%, respectively) and the heat recoverable from their combustion will significantly improve the overall efficiency. It is also noticeable that the overall water balance of the eqns. (1-3) indicates that the content of water vapour increases directly with the power.



(a)



(b)

Fig. 5. (a) Output power contributions vs. fuel utilization for $f=0.5$; (b) output power contributions vs. fuel utilization for $f=1.0$.

The sensitivity analysis (showed in Figs. 4 and 5), indicates that the electrical efficiency is affected by the electrode overpotentials and by the effect of the internal resistance. In fact, for values of power lower than 10.5 kW, an increase in the current corresponds to an improvement in the efficiency, but for higher power than this, the losses will be extreme, resulting in a worsening of the system performance.

Obviously, the overall system efficiency strongly improves if the thermal energy available in the exhaust gases is fully recovered ($f=1$). In this case, the theoretical

energy efficiency is close to 100%, with a corresponding exergy value of more than 80%. The difference (about 20%) between these efficiencies represents the unrecoverable heat.

The total output power, at the base line condition (Fig. 4(b)), is given by the contribution of the thermal and the electrical terms. The recoverable heat is very important for the cogeneration system economy and it represents a rate of the same order of the electrical energy when f is 0.5.

The H_2 represents the greatest part of the exhaust fuel (CH_4 , CO and H_2), while the CH_4 is negligible.

When the system operates at low currents, the cell must be supplied with additional heat, because the endothermic reaction of steam reforming needs more thermal energy than can be obtained from the electrochemical cell reaction. In this case the heat recovered by the combustion of the exhaust fuels can be only partially used as a thermal source for the cogeneration system because the steam reforming reaction needs the complementary heat rate.

As evident in Fig. 5, the system reaches thermal equilibrium when U_f is close to 45% and only for higher values does the cell release heat.

Conclusions

The total outlet flow, and its thermal energy density are the determining factors to the heat exchanger sizing. The mathematical analysis shows that the cathodic and the anodic streams present opposite trends with the temperature and the electrical power.

The CO yield shows a maximum for values of power between 4 and 7 kW. Beyond these values, the equilibrium of the shift eqn. (2) moves to the products because of the consumption of hydrogen. A too high power is unprofitable in a practical case, because of the excessive increase of the overpotentials and ohmic losses. The thermal energy recoverable by combustion of the unreacted fuel is an essential contribution at the overall efficiency of the system. In fact, it is of the same magnitude of the output electrical power for the system at $U_f = 60\%$ and $f = 1$. Thus, recovering completely the heat produced by the system and burning the H_2 and CO residual, it is possible to obtain an additional thermal power approximately double respect to the output electrical power.

Acknowledgements

The authors thank Dr K. Kinoshita for helpful discussions.

List of symbols

$F_{CH_4}^o$	feed rate of methane (mol/h)
$F_{H_2O}^o$	$F_{CH_4}^o S/C$ = feed rate of water (mol/h)
x, y	rate of converted CH_4 and CO in the eqns. (1) and (2) respectively (mol/h)
a, c	indices referred to the anodic and cathodic compartment
f, o, u, w, p	indices referred to the fuel, oxidant, useful, waste and produced, respectively

E°	standard electromotive force or potential when all the species involved are at unit activity (V)
R	universal gas constant, (1.987 cal/(K mol))
T	temperature (K)
P	total pressure (Pa)
F	Faraday constant, (23.06 kcal/V = 96490 C/equivalent)
n	number of transferred electrons = 2
I	current density (mA/cm ²)
S_o	effective electrodes surface (cm ²)
F_{H_2}	hydrogen flow rate = (3600I/S _o S _o)/2 96.490) (mol/h)
U_f	fuel utilization = 100(F _{H₂} /4F _{CH₄})
P_{O_2}	oxygen partial pressure (Pa)
P_{CO_2}	carbon dioxide partial pressure (Pa)
P_{H_2O}	water partial pressure (Pa)
Q_p	total output thermal power = $Q_u + \sum_w Q_w$ (W)
f	useful heat fraction = Q_u/Q_p
W	shaft work rate (W)
m	mass flow (kg/s)
h	enthalpy (J/kg)
α_E	exergy ratio for methane combustion = 0.92 [14]
η	energy efficiency
ϕ	exergy efficiency
μ	electrode overpotential (V)
R_i	specific internal resistance (Ω cm ²)
ϵ	specific exergy (J/kg)

References

- 1 M. A. Rosen, *Int. J. Hydrogen Energy*, 15 (1990) 267–274.
- 2 K. Kishita, E. Nishiyama, M. Matsumura and T. Tanaka, *Proc. Fuel Cell Technology and Applications, The Hague, Oct. 1987, Netherlands*, pp. 40–49.
- 3 T. Tanaka, M. Matsuhura, Y. Gonjo, C. Hirai, T. Okada and H. Hiyazaki, *Proc. 25th Int. Energy Conversion Engineering Conf., Reno, MN, Aug. 1990*, pp. 201–206.
- 4 T. G. Benjamin, E. H. Camara and L. G. Marianowki, *Handbook of Fuel Cell Performance, DOE Contr. EC-77-C-03-1545*, IGT, Chicago, IL, 1980.
- 5 S. Freni, N. Giordano and S. Cavallaro, *J. Appl. Electrochem.*, 20 (1990) 804–810.
- 6 K. Sato, T. Tanak and T. Murahashi, *Proc. 1990 Fuel Cell Seminar, Phoenix, AR, 1990*, pp. 40–43.
- 7 D. L. Curtis, *Proc. 8th World Hydrogen Energy Conf., Honolulu (USA), 1990*, pp. 49–58.
- 8 J. R. Rostrup-Nielsen, *Steam Reforming Catalyst*, Danish Tech. Press Inc., Copenhagen, 1975.
- 9 T. Murahashi, *Proc. Second Symposium of MCFC, Kyoto, Japan, 1988*, pp. 50–53.
- 10 G. Wilemski, J. Mitteldorf and J. Simons, *Diagnostic Fuel Cell Model, PSI Contr. DE-AC05-79ET-15403*, Physical Sciences Inc., Woburn, MA, 1982.
- 11 T. Mori, K. Higashiyama, S. Yoshioka, T. Kobayahi and S. Itoh, *J. Electrochem. Soc.*, 136 (1989) 2230–2234.
- 12 R. A. Gaggioli and P. J. Petit, *Chemtech*, 7 (1977) 496–506.
- 13 K. Kinoshita, F. R. McLarson and E. J. Cairns, *Fuel Cells, A Handbook*, US Department of Energy—Office of Fossil Energy, Morgantown, 1988.
- 14 H. B. Vakil and J. W. Flock, Closed loop chemical systems for energy storage and transmission, Prepared by General Electric under ERDA Contract no. EY-76-C-02-2676, US department of Energy, Washington, DC, 1978.